MEASUREMENT OF DNI ANGULAR DISTRIBUTION WITH A SUNSHAPE PROFILING IRRADIOMETER

Ragini Kalapatapu[1], Matteo Chiesa[1], Peter Armstrong[2] and Stefan Wilbert[3]

[1] Ragini Kalapatapu- Graduate Student, MSc in Mechanical Engineering, Prof. Dr. Matteo Chiesa - Associate Professor, Material Science and Engineering, Masdar Institute of Science & Technology

[2] Prof. Dr. Peter Armstrong, Associate Professor, Masdar Institute of Science & Technology, Masdar City, Abu Dhabi 54224, UAE Phone: +971 2810 9151, E-Mail: parmstrong@masdar.ac.ae

[3] Stefan Wilbert- Dipl.-Phys, German Aerospace Center (DLR), Solar Research, Plataforma Solar de Almería (PSA)

Abstract
A low cost, field-deployable instrument for retrieving the radial profile of solar radiance across the sun's disk and through the circumsolar region is described. A prototype of the Sunshape Profiling Irradiometer (SPI) has been built by modifying a stepping-motor-based Rotating Shadowband Irradiometer (RSI) with straightforward changes to the control and data collection program and mechanical modifications that are novel but simple. A slit, rather than circular, receiver aperture is disposed on the band axis such that penumbra crosses the aperture with a very small angular displacement of the shadowband. Because a single detector with diffusing fore-optic is used to generate the sunshape profiles, calibration and soiling problems commonly associated with high resolution cameras are avoided. The circumsolar ratio (CSR) of the generated SPI trajectory is estimated by finding the best match of the normalized measured profile to the family of simulated profiles using a single-parameter model. Results of CSRs obtained by this inverse method are compared to the broadband CSR given by the sun aureole measurement system and sun photometer. Applications of SPI include optimizing concentration ratios of CSP plants based on local CSR distribution, adjusting normal-incidence- and IAM-test results for the direct normal irradiation (DNI) within a concentrator's acceptance angle, and inferring aerosol distributions for climate studies or as input to remote sensing models.

Keywords: sunshape retrieval, circumsolar, aerosol, scattering, DNI, CSR, angular distribution

1. Introduction

Measurement of the angular distribution of radiation from the circumsolar region (sunshape) is a longstanding problem in solar resource assessment yet to be satisfactorily addressed. The combination of Rayleigh and (predominantly) Mie scattering creates a specific spatial and spectral energy distribution which depends on zenith angle and the atmospheric conditions at a particular time and location. A tracking pyrheliometer, the standard instrument for measuring direct normal irradiation (DNI), responds to radiation from the disk and a fixed portion of the circumsolar region of usually 2.5-3˚ half angle but provides no information about angular distribution [1]. The angular distribution of radiation has been shown to be only very roughly correlated with DNI [2]. A more precise knowledge of the angular distribution is useful in a number of applications.

- To optimize the receiver aperture of a concentrating solar power (CSP) system and properly estimate annual yields one needs, in addition to standard DNI, the angular distribution at each analysis time step [3].
- *Real-time* sunshape data may be useful for improving the performance of photogrammetric heliostat aiming algorithms [4].
- Concentrator normal-incidence performance tests and transverse and longitudinal incident angle modifier function tests require accurate measurements of sunshape.
- Sunshape can be used to estimate aerosol optical depth (AOD), size distribution of aerosols, and for validation of radiative the transfer models essential to climate research and global or regional weather forecasting models.

Existing and previously used high-resolution circumsolar and sky mapping instruments are expensive, data intensive, and too labor intensive for long term or remote deployment. We are developing a Sunshape Profiling Irradiometer (SPI) intended to provide brightness distributions at high sampling rates in a simple low cost instrument that requires no more maintenance than a RSI. This paper describes the instrument's design, an inverse method of retrieving CSR from the SPI signal, and verification of instrument and method against data from a SAM camera [5].

2. SPI instrument description

A stepper motor driven Rotating Shadowband Irradiometer (RSI) has been modified to build a prototype instrument [6]. In the first SPI prototype we have retained the shading mechanism of the conventional RSI wherein a shadowband rotates about a polar axis on which the detector aperture is disposed. The main modification entails use of an optical slit receiver with slit azimuth = 0^o and tilt equal to latitude of the location. The receiver aperture is situated exactly on the band-motor (polar) axis as shown in Figure 1. A standard Li-Cor PY-200 receiver/detector is modified by covering its circular diffusing aperture with a piece of black foil into which a very narrow rectangular slit is cut along the axis line. Use of a slit sharpens the corners of the trough-like SPI trajectory which in turn reduces sensitivity of the retrieved brightness distribution to noise and other measurement errors. The receiver orientation is modified in order to eliminate the angular movement of the shadow cast by the band on the receiver with time of the day as illustrated in Figure 1.

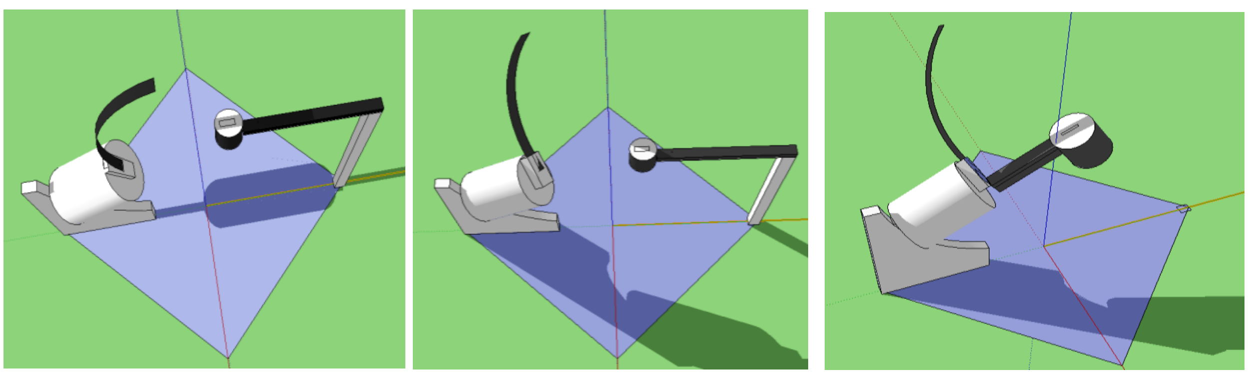

Fig. 1: Shadow analysis a) horizontal receiver at noon b) after noon c) tilted receiver

The original RSI [7] used half stepping to achieve a resolution of 0.45^o or 800 steps per revolution in half-step mode. Effective resolution of 800*27= 21600 micro steps/revolution may be achieved with the SPI by scanning the circumsolar region 27 times in under 2 minutes. The 61 measurements from each sweep are interleaved to create the same sequence of 61*27=1647 that would be observed by 0.017^o steps taken in a single sweep.

To estimate the accuracy of sunshape retrieval, simulated signals with additive Gaussian noise were analyzed [8]. While these numerical experiments show that more measurements per sample are better, in practice shadowband position error is a problem. Further experience with SPI prototypes will determine the best angular resolution.

3. CSR retrieval with inverse Buie model

Grether [9] observed that sunshape profiles were almost linear in log-log space the circumsolar region (6^o field of view). Neumann compared LBL [10] and DLR sunshapes to find that they are similar, within normal (conditional on CSR) variations and instrument uncertainty, as shown in Figure 3. Buie [11] proposed empirical formulas for slope and intercept as functions of CSR, resulting in the following brightness model:

$$\phi(\theta) = \begin{cases} \cos(0.326\theta)/\cos(0.308\theta), & (0 \le \theta \le \theta_s) \\ e^{\kappa}\theta^{\gamma}, & (\theta > \theta_s) \end{cases} \qquad (1)$$

where θ_s = half-angle subtended by radius of the solar disk,

$$\gamma = 2.2\ln(0.52 \cdot CSR) \cdot CSR^{(0.43)} - 0.1 \text{ and}$$

$$\kappa = 0.9\ln(13.5 \cdot CSR) \cdot CSR^{(-0.3)} \tag{2}$$

The normalized brightness distribution, $\phi(\theta)$ thus depends on only one parameter, CSR.The constants in the expressions for κ and γ were obtained by least squares using LBL and DLR brightness data out to 2.5˚ such as that presented by [2] reproduced here in Figure 3. The constants (2) were selected such that the definition of CSR is approximately satisfied:

$$CSR \approx \frac{\int_{\theta_S}^{2.5^\circ} \sin(\theta)\phi(\kappa(CSR), \gamma(CSR), \theta) d\theta}{\int_{0}^{2.5^\circ} \sin(\theta)\phi(\kappa(CSR), \gamma(CSR), \theta) d\theta} \tag{3}$$

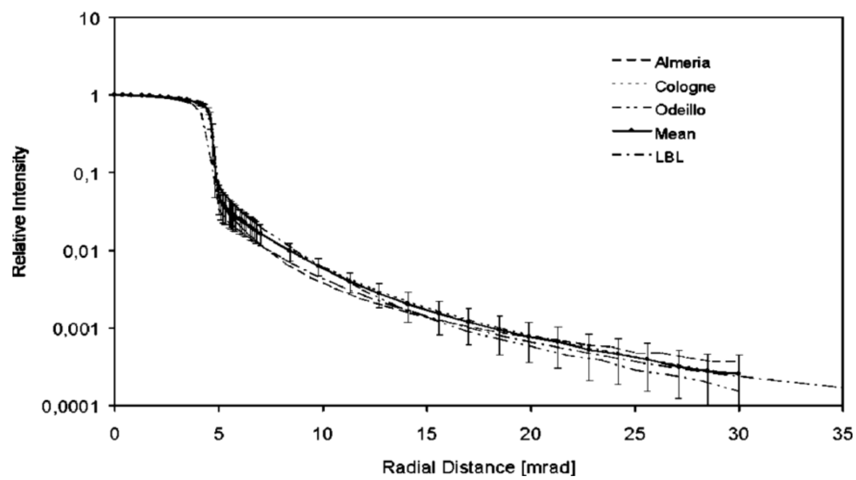

Fig. 2: LBL and DLR sunshapes for CSR=0.10 with uncertainty bands [2]

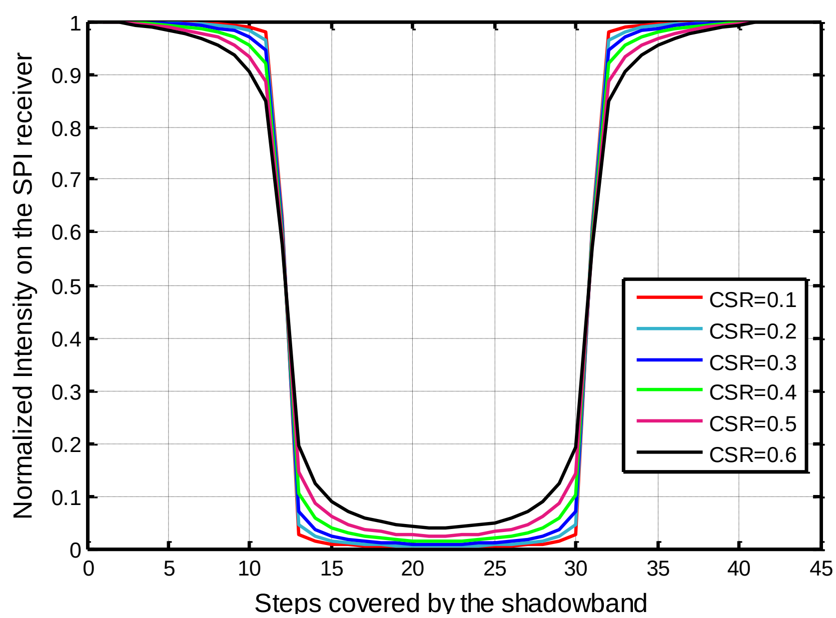

Fig. 3: Family of simulated SPI signals, S (CSR, w), generated at different CSRs

The CSR corresponding to the simulated signal that best matches the measured SPI trajectory is identified by comparing the residuals of the simulated signals with respect to the measured signal using two coefficients, ξ_o and ξ_1, to denormalize each simulated trajectory.

$$I_{T,measured}(j) = \xi_o + \xi_1 S(CSR, j) + n(j) \tag{4}$$

where $S(CSR,j)$ is the simulated signal for band position j obtained by integrating the modeled circumsolar region for a given circumsolar ratio, CSR, and $n()$ is the residual vector to which both model and measurement errors contribute. Integrations used to generate the family of curves $S(CSR,j)$ are developed in Appendix A.

The denormalizing coefficients ξ_o and ξ_1 are estimated by ordinary least squares for the simulated SPI signal corresponding to each candidate CSR. ξ_o represents the diffuse irradiation from outside the circumsolar region that falls on the tilted receiver including a portion of ground reflected radiation. Figure 4 shows the offset (ξ_o) between the measured SPI trajectory and the simulated signal pertaining to a particular CSR. This offset is necessary because the Buie model does not specify brightness outside of the circumsolar region. The candidate CSR that gives the least sum of squared deviations, $n \cdot n$, between the measured SPI trajectory, $I_{T,\text{measured}}(j)$, and the denormalized simulated signal, $\xi_o + \xi_1 S(CSR,j)$ (3), is an estimate of the true CSR.

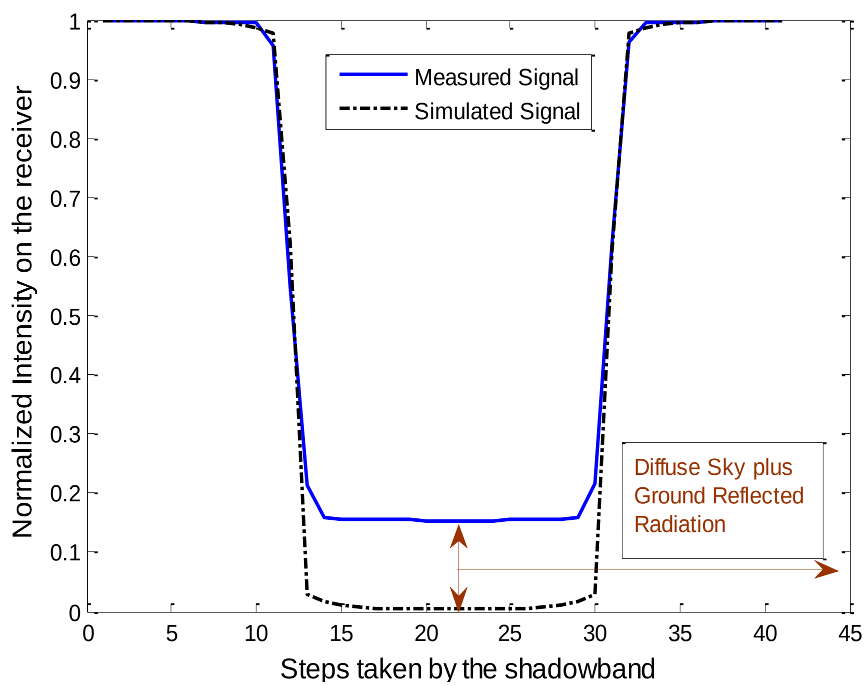

Fig. 4: Measured and Simulated SPI Trajectories

Figure 5 shows the RMS deviations of the simulated curves for each candidate CSR with respect to SPI trajectories measured at 12:25, 13:31, 14:35 and 15:27 on 27 Feb 2012.

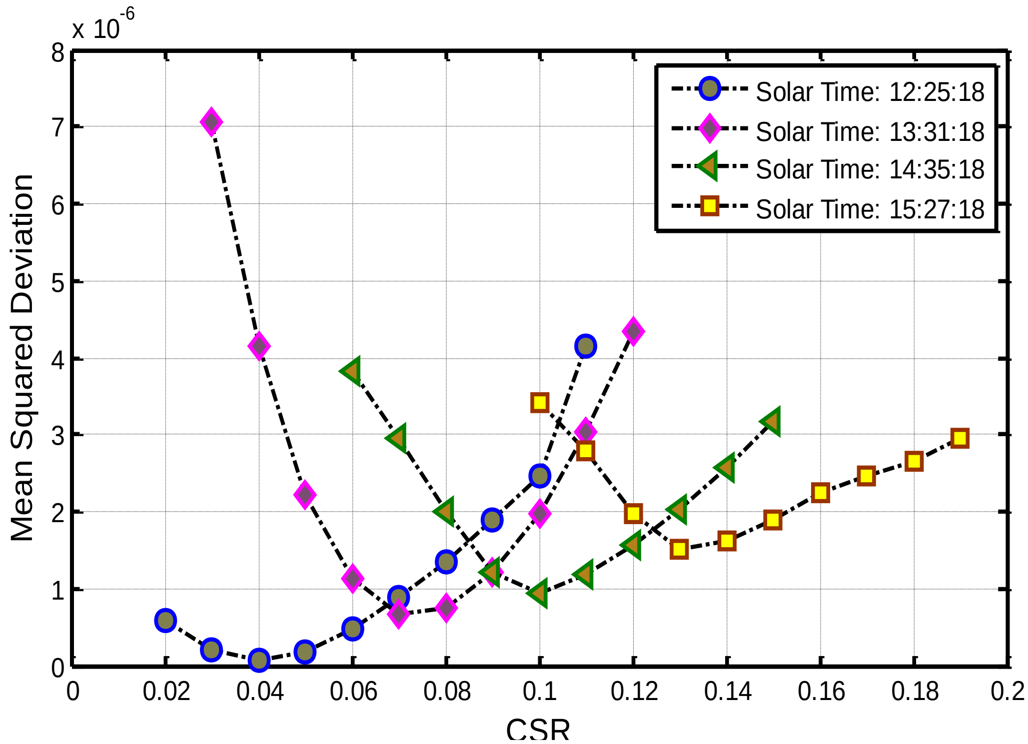

Fig. 5: MSE plot of the family of simulated signals with respect to the instantaneous SPI trajectory measured on Feb-27, 2012.

4. Results (CSR estimated from SPI data by inverse model)

The prototype instrument was deployed for several days in order to test its measuring capability and the retrieval method described in the previous section. Under clear low aerosol sky conditions, the predicted CSRs are found to be very low (below 10%) with high DNI ranging from 750-854 W/m^2. Figure 6 illustrates the variation of CSR with time of the day (every ten minutes) under the very clear sky conditions of Feb-27.

Figure 7 illustrates the variation of CSR with time on Mar-01, 2012 when conditons were noticably dusty/hazy and the peak DNI attained on this day was only 451W/m^2. Under these dusty conditions CSR may reach 60% and the aureole half-angle can be much higher than the 43.6 mrad (2.5^o) range of LBL sunshape data on which (2) is based.

The CSRs averaged every half an hour on Feb-27, 2012 are compared with the averaged half hour DNIs of the same day as shown in figure 8. We have observed on exemplary clear days that CSR increases with decrease in DNI. However Neumann has found that in general CSR does not depend on the DNI in a simple monotonic way [12].

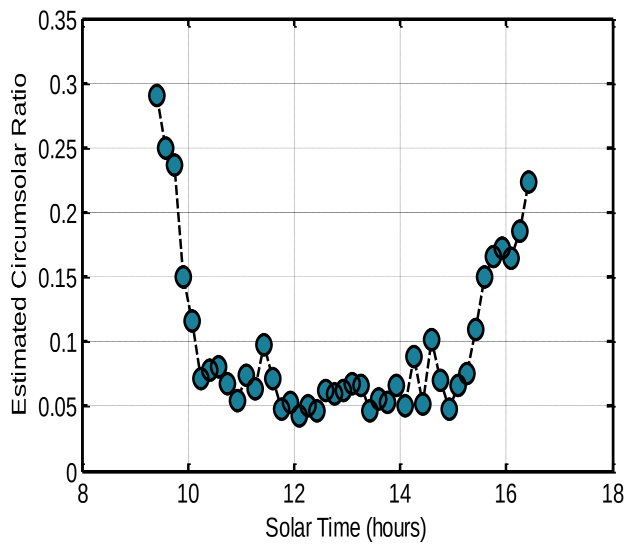

Fig. 6: Predicted CSR values on a clear day, Feb-27

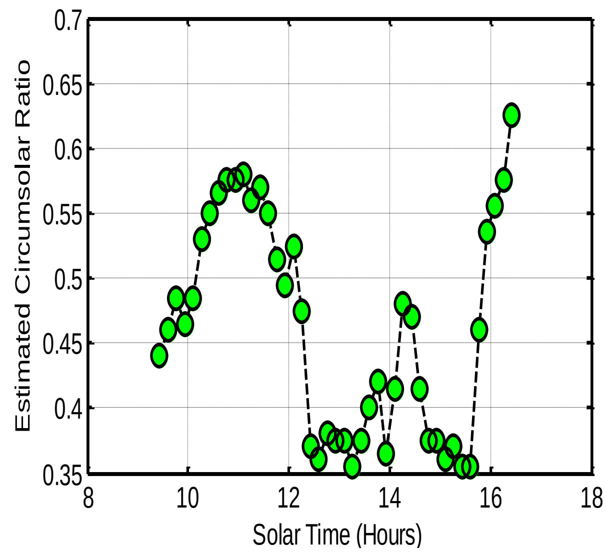

Fig. 7: Predicted CSR values on a dusty day, Mar-01

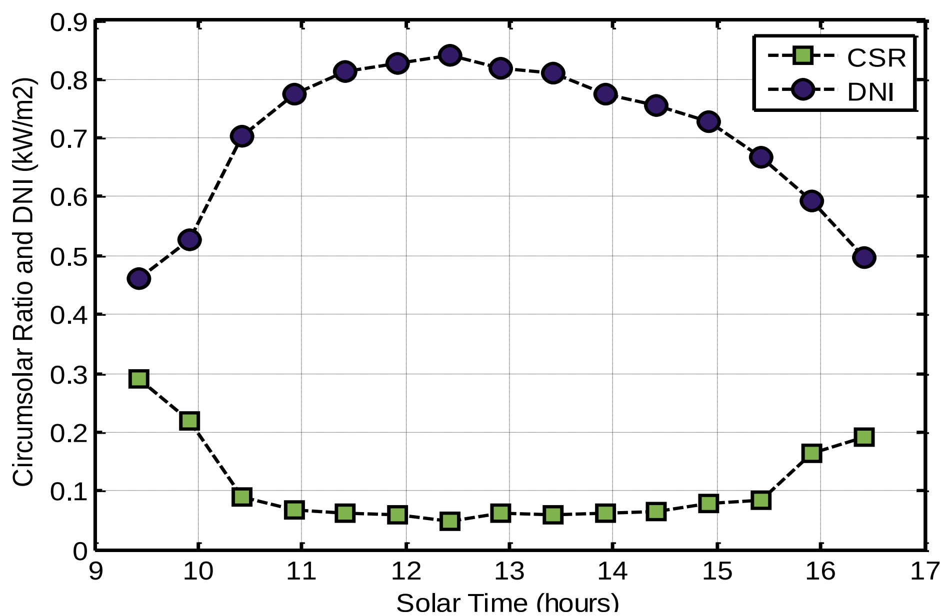

Fig. 8: DNI (kW/m^2) and CSR (dimensionless) on Feb-27, a clear day

4.2 Least squares coefficients from the inverse model

In the retrieval procedure, the first denormalization coefficient, ξ_o is expected to be lower than the total diffuse irradiation on a horizontal receiver except in rare cases where there is a large reflected component from the foreground within the receiver's field of view.

The second ξ_1 is proportional to the sum of DNI and circumsolar radiation incident on the receiver. Hence ξ_1 is expected to be always more than the projected DNI/GHI because the circumsolar region (as defined in appendix A) is larger than the FOV of a conventional DNI measuring instrument. The expected relations between the denomalization coefficients and the measured DHI and projected DNI are confirmed in figure 9.

The ground reflected part includes both DNI and DHI contributions and, if ρ_g is known, can be evaluated by standard models for tilted collectors [13]. Thus the SPI can work as a conventional RSI, apart from its main function of measuring the sunshapes, if a reasonable estimate of foreground albedo available.

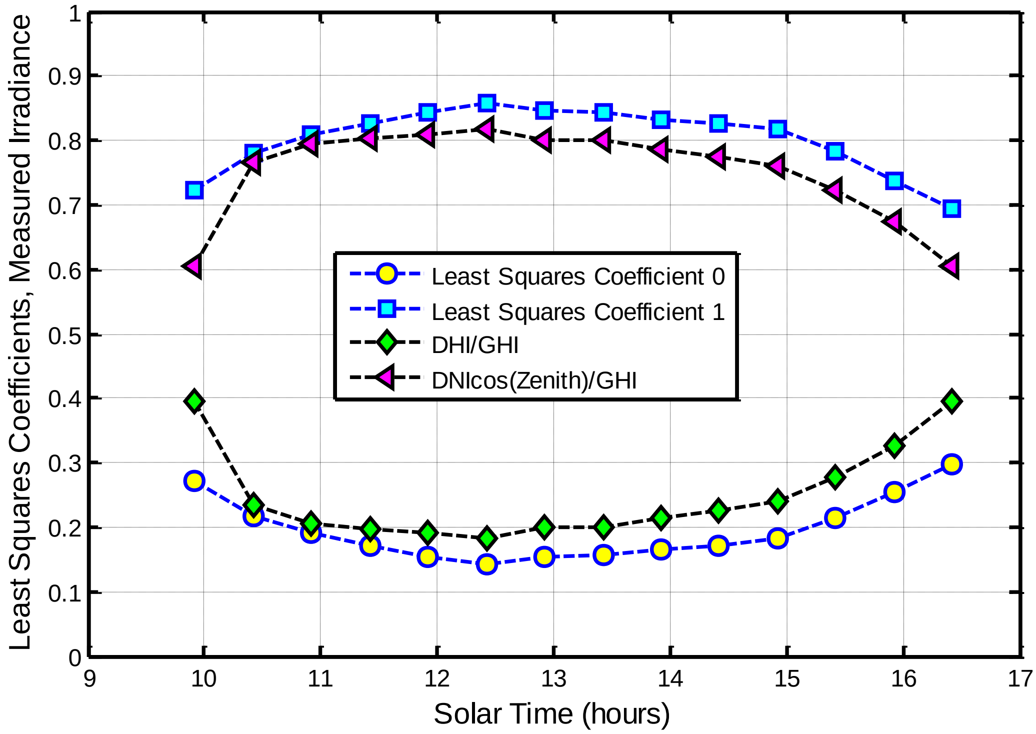

Figure 9: Least squares coefficients ξo and ξ_1, normalized to I_T, and RSI-measured components of Solar Irradiance, normalized to GHI (Feb-27, 2012).

4.3 Verification of the SPI-estimated CSRs with SAM and sun photometer

The Sun and Aureole Measurement (SAM) System is a research instrument that provides accurate and high resolution brightness maps of the solar disk and aureole up to a large half acceptance angle using calibrated CCD cameras. The CSRs obtained by the inverse model from the SPI measurements are compared with the broadband CSRs estimated from the SAM aureole profiles and sun photometer data taken at the same location on the Masdar irradiometer platform in Abu Dhabi. CSRs estimated from the SPI-inverse Buie model follow the trends of CSRs obtained by the SAM during 3 days of post-commissioning operation in Sep-2012. CSR trends and general agreement of SPI and SAM results are encouraging. Analysis of recent data collected after SPI and SAM operational improvements will hopefully provide further validation of the SPI instrument and sunshape retrieval method.

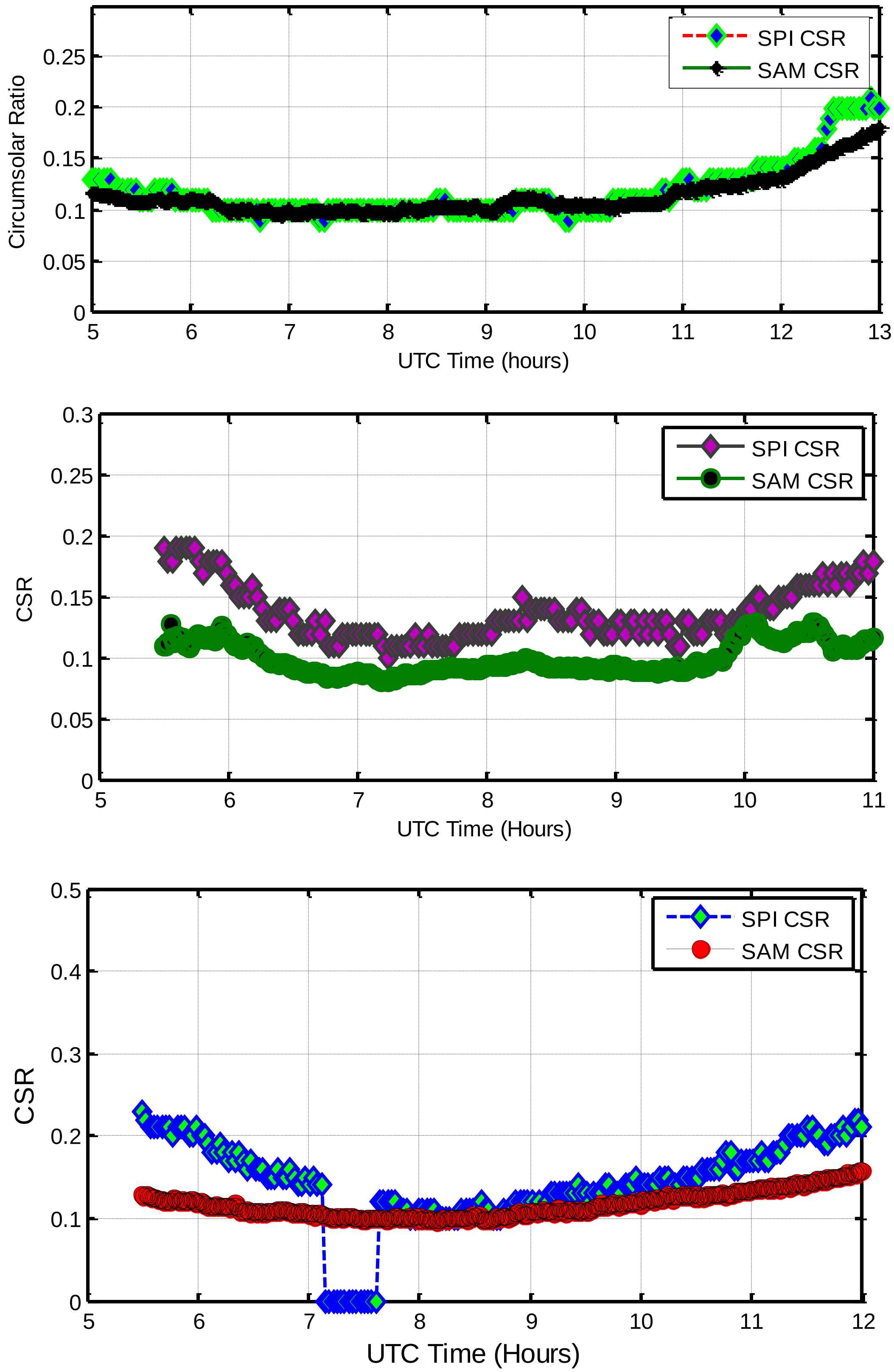

Fig. 10: CSRs estimated from SAM and SPI at 2 minute intervals on 5, 6 and 7 September, 2012.

5. Conclusion

This paper describes initial efforts to develop and validate performance of a new instrument for measuring the circumsolar brightness profile. We have found that the CSR can be estimated from the trough-like signal trajectories of the SPI using an inverse Buie model. Least squares regression is performed on the measured signal against a family of simulated curves with varying CSRs. The simulated curve with least mean squared error corresponds to the estimated CSR. The coefficient of least squares (ξ_o) pertaining to the sky radiation plus part of ground reflected radiation falling on the receiver is observed to be approximately proportional to the DHI outside the sunshape analysis region. The other coefficient (ξ_1) is observed to be proportional to the DNI plus circumsolar contributions with appropriate cosine corrections within the sunshape analysis region. The CSRs obtained from the SPI trajectories with the inverse Buie model are compared with the broadband CSRs obtained from the SAM based system and are found to agree reasonably well when the sun-receiver angle of incidence is less than about 50˚.

Further work is needed to reduce receiver cosine error. Basis functions that are more general than the Buie model are also being tried. For example the log-log slope and intercept, γ and κ, can be independently estimated to obtain a 2-parameter description of angular distribution. By direct inversion a non-parametric profile can, in principle, be retrieved as well.

In future, use of multiple filter detectors are planned to give distinct angular distributions from which further information about aerosol distributions can be inferred [14]. Also, micro-stepping of the band motor will eliminate multiple sweeps, shorten the sampling time and reduce vibration of occulting band.

A low-cost, low-maintenance automatic instrument deployed at a large number of sites will lead, in due time, to a large database (~100,000 per site per year) of sunshapes. Angular distributions of circumsolar radiation will enable CSP yield estimates and design optimizations that are more accurate than estimates based on current DNI data.

Acknowledgements

The sunshape project has been supported by MIST/Masdar Initiative/AbuDhabi Government. Patent application costs were substantially defrayed by generous support from the Abu Dhabi Patent Harvesting Program. Atul Jadhav and WeiDong Xiao assisted with micro-step band control. The enthusiastic and skilled technical support of M'd Tauha Ali is gratefully acknowledged as are the conscientious efforts of a number of LENS staff who volunteered for semi-weekly irradiometer cleaning. We especially thank Olaf Goebel for encouraging this line of research.

Appendix A. Evaluation of SPI trajectory forward model by integration over sunshape analysis region

Buie's equations may be used to produce a normalized SPI signal that is a function of CSR only. The procedure requires integrations over the circumsolar analysis region shown in Fig. A-1 where ω = relative hour angle, α_o = declination and $\Delta\omega$ = bandmotor step size. The average intensity I_ω of a given strip as viewed from the receiver is:

$$I_\omega = \int_{\alpha_1}^{\alpha_2} \phi(\omega, \alpha, CSR, \theta)\cos(\theta)\cos(\alpha)\Delta\omega d\alpha \qquad \text{(A1)}$$

where $\cos(\theta) = \cos(\alpha - \alpha_o)\cos(\omega - \omega_o)$. From the receiver, the shadowband's width subtends 148.35 mrad (8.5°); its half angle may be expressed in terms of micro-steps as n and the band position as j while t is the total number of strips and ξ_0 and ξ_1 are the denormalizing coefficients to be obtained by least squares. In case of a receiver with finite width, the sky and band view factors vary from one edge of the receiver to the other. Hence, a weight function is applied across the width, m, of the slit receiver The simulated signal is thus given by:

$$I_{measured}(j) = \xi_0 + \xi_1 \left\{ \sum_{\omega=1}^{t} I_\omega - \sum_{i=j-n-m}^{j-n} \frac{i-n-m}{m} I_\omega - \sum_{i=j+n}^{j+n+m} \frac{i-n}{m} I_\omega \right\} \qquad \text{(A2)}$$

where $\omega = \omega_o + i\Delta\omega$. The expression in braces is the normalized simulated irradiation trajectory from the circumsolar analysis region which, for simplicity, we may denote by $S(CSR,j)$, thus the irradiance signal is:

$$I_{measured}(j) = \xi_o + \xi_1 S(CSR, j) \tag{A3}$$

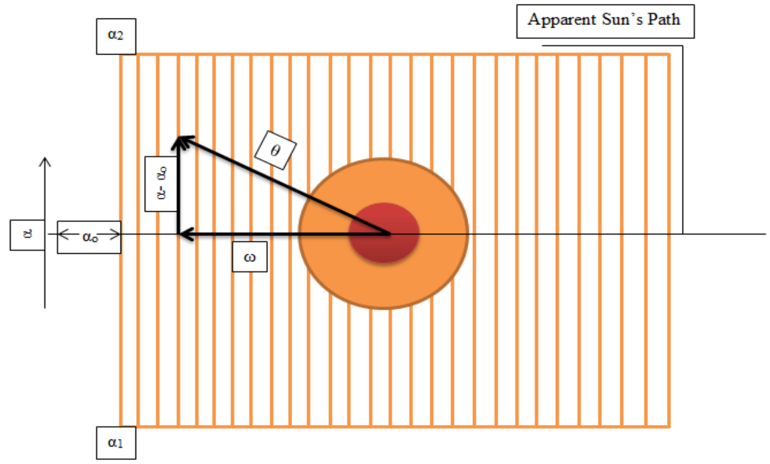

Figure A-1: Equirectangular projection of CS region divided by shadowband micro-steps (not to scale)

References

[1] T. Stoffel, D. Renne', D. Myers, S. Wilcox, M. Sengupta, R. George and C. Turchi, "Concentrated Solar Power: Best Practices Handbook for the Collection and Use of Solar Resource Data," National Renewable Energy Laboratory, Golden, Colorado, 2010.

[2] A. Neumann, A. Witzke, J. A. Scott and S. Gregor, "Representative Terrestrial Solar Brightness Profiles," *Journal of Solar Energy Engineering*, vol. 124, pp. 198-204, 2002.

[3] P. Bendt, A. Rabl, H. Gaul and K. A. Reed, "Optical Analysis and Optimization of Line Focus Solar Collectors," Solar Energy Research Institute, Colorado, 1979.

[4] Y. Gilon, I. Kroizer and G. Kroyzer, "Method and Control System for operating a Solar Power Tower System". Patent 20120024282, 2008.

[5] S. Wilbert, B. Reinhardt, J. DeVore, M. Roger, R. Pitz-Paal and C. Gueymard, "Measurement of Solar Radiance Profiles With the Sun and Aureole Measurement System (SAM)," in *Solar Paces*, Granada, 2011.

[6] P. R. Armstrong, R. Kalapatapu and M. Chiesa, "Slit-optics, polar-axis shadowband radiometer and method for its use in mapping circumsolar radiation". UAE 2011.

[7] J. J. Michalsky, J. L. Berndt and G. J. Schuster, "A Microprocessor- Based Rotating Shadowband Radiometer," *Solar Energy*, vol. 36, no. 5, pp. 465-470, 1986.

[8] R. Kalapatapu, P. R. Armstrong and M. Cheisa, "Rotating Shadowband for the Measurement of Sunshape," in *Solar Paces 2011*, Granada, 2011.

[9] D. Grether, D. Evans, A. Hunt and M. Whalig, "Measurements and Analysis of Circumsolar Radiation," Lawrence Berkeley Laboratory, Report No.10243, 1979.

[10] J. Noring, D. Grether and A. Hunt, "Circumsolar Radiation Data: The Lawrence Berkeley Laboratory Reduced Data Base," NREL Rep. TP-262-4429, Berkeley, 1990.

[11] D. Buie, Optical Considerations in Solar Concentrating Systems, University of Sydney, Sydney: PhD Thesis, 2004.

[12] A. Neumann, B. von der Au and P. Heller, "Measurements of Circumsolar Radiation at the Plataforma Solar (Spain) and in Cologne (Germany)," in *Proc. of Int. Solar Energy Conf. Solar Engineering*, Albuquerque, 1998.

[13] J. A. Duffie and W. A. Beckman, Solar Engineering of Thermal Processes, John Wiley & Sons, 2006, Third Edition.

[14] O. Dubovik and M. D. King, "A flexible inversion algorithm for retrieval of aerosol optical properties from sun and sky radiance measurements," *J.Geophysical Res.*, vol. 105, no. D16, pp. 673-696, 2000.